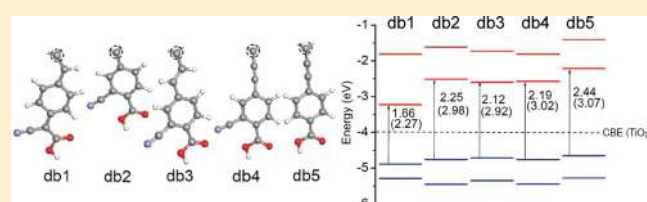


# Design of Dye Acceptors for Photovoltaics from First-Principles Calculations

Sheng Meng,<sup>\*,†</sup> Efthimios Kaxiras,<sup>‡</sup> Md. K. Nazeeruddin,<sup>§</sup> and Michael Grätzel<sup>§</sup><sup>†</sup>Beijing National Laboratory for Condensed Matter Physics, and Institute of Physics, Chinese Academy of Sciences, 100190 Beijing, China<sup>‡</sup>Department of Physics and School of Engineering and Applied Sciences, Harvard University, Cambridge, Massachusetts 02138, United States<sup>§</sup>Laboratory of Photonics and Interfaces, Institute of Chemical Sciences and Engineering, Swiss Federal Institute of Technology (EPFL), CH-1015 Lausanne, Switzerland

**ABSTRACT:** We investigate a set of donor- $\pi$ -acceptor (D- $\pi$ -A) dyes with new acceptor groups for dye-sensitized solar cells, using time-dependent density-functional-theory calculations of the electronic structure and optical absorption. We considered three types of modifications on existing dye structures: (i) replacement of the side cyano group (CN) on the molecular anchor, (ii) insertion and alteration of the intermediate spacer groups, and (iii) modification of the number and positions of cyano CN groups on a phenyl-ring spacer. We find that with these modifications, the dye electronic levels and corresponding optical absorption properties can be gradually tuned, rendering possible the identification of dyes with desirable structural, electronic, and optical properties. For example, dyes with phenyl and CN-substituted phenyl groups are promising candidates for red light absorption and high molar extinction coefficients.



Among current renewable energy solutions, dye-sensitized solar cells (DSCs, also referred to as “Grätzel cells”), provide an inexpensive and environmentally friendly alternative for sunlight-to-electricity conversion.<sup>1–3</sup> In this type of device the dye molecules are used to sensitize transparent oxide semiconductors (such as TiO<sub>2</sub> and ZnO), performing a crucial function in the harvesting of infrared-visible light, which comprises 95% energy of the solar spectrum. Synthetic dyes containing metal ions (usually expensive transition metals such as Ru) have been widely used and have led to the highest efficiency achieved for such devices, approaching 12%.<sup>3</sup> Purely organic, metal-free dyes<sup>4–10</sup> are also promising, given their wide availability, benign environmental effects, and low cost. The challenges for developing all-organic dyes are to widen their relatively narrow adsorption band in the visible region and to raise their low efficiency.<sup>3,6</sup> Recent progress toward meeting these challenges includes synthesizing electron-rich donor- $\pi$ -acceptor (D- $\pi$ -A) dyes to achieve higher molar extinction coefficients, thus reducing film thickness and electronic loss in devices; this strategy has produced encouraging results with energy conversion efficiency exceeding 10%.<sup>11</sup>

A novel D- $\pi$ -A structure for effective all-organic dyes involves the donor and acceptor connected through a molecular bridge conductor ( $\pi$  group), and the acceptor is directly bound to the semiconductor surface. In this structure, upon excitation by light, electrons in the highest occupied molecular orbitals (HOMOs) originally distributed around the donor group are promoted to the lowest unoccupied molecular orbitals (LUMOs) which are centered around the acceptor. This excitation process effectively

pushes extra electrons to the acceptor part of the dye and leaves holes on the donor part. An important aspect of the D- $\pi$ -A structure is the proximity between the acceptor and the semiconductor surface, which are mutually bound through covalent and/or hydrogen bonds. This allows ultrafast transfer of excited electrons to the conduction bands of the semiconductor<sup>12,13</sup> and leads to efficient electron–hole separation and ultimately electricity generation. The performance of an organic dye in real devices depends sensitively on its structure and electronic/optical properties, such as the binding stability, the band alignment, and the absorption maximum and intensity. Tuning these parameters can greatly enhance the device performance, eventually leading to large-scale implementation of DSCs for solar energy conversion. Laboratory development of D- $\pi$ -A dyes often invokes a trial-and-error approach which requires extensive chemical synthesis and expensive materials processing, a slow and laborious process. In this regard, theoretical screening of potential organic dyes using state-of-the-art first-principles calculations holds great promise to significantly reduce the cost of developing efficient dyes and to expedite discovery of new ones.

In principle, rational design and analysis of each component of a D- $\pi$ -A organic dye, including the donor group, the molecular conductor, and the acceptor group, is desirable in order to further develop more efficient organic dyes for DSCs. In this work we

Received: February 19, 2011

Revised: March 23, 2011

Published: April 18, 2011

investigate the influence of the acceptor group of the D- $\pi$ -A dye on its electronic and optical properties, since it connects the dye to the semiconductor and plays a critical role for dye anchoring, optical absorption, and electron-transfer processes. Our strategy is to test systematically the influence of chemical group substitution on the electronic and optical properties of the dyes. Chemical groups of different electronegativity, size, and shape, and at different sites, have been investigated. In particular, we considered mainly three types of modifications on the existing dye structures: (i) replacement of the  $-\text{CN}$  group of cyanoacrylic side with other elements or groups, giving a group of new dyes which we label da- $n$  (with  $n = 1-5$ , an index); (ii) alteration of the intermediate molecular spacer groups (the dye group labeled db- $n$ ); and (iii) modification of the number and position of  $-\text{CN}$  on the phenyl-ring spacer group (the dye group labeled dc- $n$ ). We found that with these modifications of the dye acceptor group, the electronic levels, and corresponding optical absorption properties can be gradually tuned, and as a consequence dyes with desirable electronic and optical properties can be identified. The best candidates for high extinction coefficients and long-wavelength absorption turn out to be dyes with a novel phenyl spacer between the carboxylate–cyanoacrylic anchoring group and the dithiophene conductor (db1) and that with a CN-substituted phenyl ring (dc5). These dyes have an extremely large oscillator strength (2.443 for db1 and 2.176 for dc5) at a long wavelength in vacuum (546 nm for db1 and 523 nm for dc5) and in solution (594 nm for db1 and 547 nm for dc5).

We address first certain important computational issues, to establish the reliability of the results reported below. Since the all-organic dyes used in experiments are relatively large in size, involving  $\sim 100$  atoms, extensive use of high-accuracy ab initio quantum chemistry methods is usually prohibitive due to the heavy computational cost involved and the poor scaling ( $\sim N^6$ ,  $N$  being the number of electrons). Calculations of electronic properties and optical absorption based on time-dependent density functional theory (TDDFT)<sup>14,15</sup> have proven a valuable tool because of their high efficiency, reasonable accuracy, and good scalability. However, commonly employed approximate density functionals for the exchange–correlation (XC) energy are not suitable for charge-transfer excitations, Rydberg states, and multiple excitations, mostly due to the lack of asymptotic  $1/r$  behavior of Coulomb interactions;<sup>16</sup> the use of such functionals leads to problematic predictions for optical excitations. Significant progress has been made recently by including self-interaction corrections in hybrid functionals,<sup>17–19</sup> to properly account for the long-range charge-transfer excitations while retaining a reliable description of short-range correlation interactions. Results of this approach compare favorably to results obtained from high-level wave function-based ab initio quantum calculations.<sup>20,21</sup>

Our calculations were performed within the framework of density-functional theory (DFT) for structure optimization<sup>14</sup> and TDDFT for excited states and optical absorption,<sup>15</sup> using the SIESTA<sup>22</sup> and Gaussian<sup>23</sup> codes. For structure optimization, we use pseudopotentials of the Troullier–Martins type<sup>24</sup> to model the atomic cores, the PBE form of the exchange–correlation functional,<sup>25</sup> and a local basis set of double- $\zeta$  polarized orbitals (13 orbitals for C, N, O, F, and S; 5 orbitals for H). An auxiliary real space grid equivalent to a plane-wave cutoff of 100 Ry is used for the calculation of the electrostatic (hartree) term. A molecular structure is considered fully relaxed when the magnitude of forces on the atoms is smaller than 0.02 eV/Å. Optical absorption

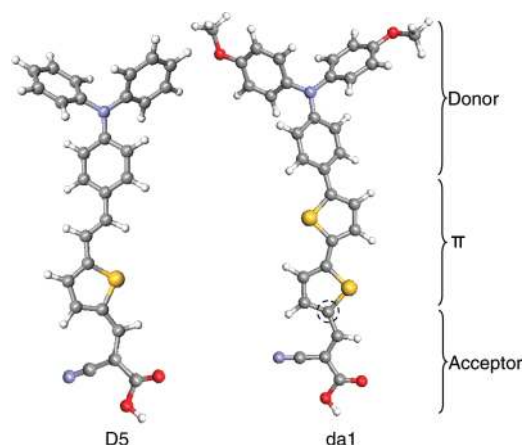


**Figure 1.** Optimized atomic structure of the donor- $\pi$ -acceptor dyes D5 and da1; gray, red, blue, yellow, and white spheres represent C, O, N, S, and H atoms, respectively. The donor, acceptor, and  $\pi$  conductor of the dye are denoted. The dashed circle marks the carbon atom connecting the acceptor part and the  $\pi$  bridge.

results are obtained from TDDFT simulations within linear response at fixed dye geometry in the gas phase corresponding to isolated molecules, and in solution employing the polarizable continuum model.<sup>26</sup> We use the 6-31G(d) basis set throughout this paper, which has been shown to yield negligible differences in electron density and energy accuracy compared with basis sets that include additional diffuse functions.<sup>21</sup> We checked carefully the effect of geometry optimization procedures on the final atomic structure and excitation energies. Geometries optimized with Becke's three-parameter and Lee–Yang–Parr's gradient-corrected correlation hybrid functional (B3LYP) and 6-31G(d) basis sets show very small differences in bond lengths ( $\sim 0.001$ – $0.02$  Å) and bond angles ( $< 1^\circ$ ) compared to results obtained using PBE functionals and the atomic basis sets in SIESTA. More importantly, the HOMO–LUMO energy gap differences are within  $\sim 0.1$  eV for the two geometries in both ground-state and excited-state calculations. Such a variation in energy is acceptable since it is within the typical accuracy of DFT and TDDFT calculations of optical properties. For checking the reliability we use a variety of different XC functionals, including PBE, B3LYP, CAM-B3LYP,<sup>18</sup> and  $\omega$ B97X<sup>19</sup> in TDDFT based on the adiabatic approximation. The latter two are employed to correct the energies for charge-transfer excitations, which are dominant in the dyes we are considering. The spectrum is obtained using the following expression based on the calculated excitation energies ( $\omega_i$ ) and oscillator strengths ( $f_i$ )

$$\varepsilon(\omega) = 2.174 \times 10^8 \sum_i \frac{f_i}{\Delta} \exp \left[ -2.773 \frac{(\omega - \omega_i)^2}{\Delta^2} \right] \quad (1)$$

where  $\varepsilon$  is the molar extinction coefficient given in units of  $\text{M}^{-1} \text{cm}^{-1}$ , the energies  $\omega$ ,  $\omega_i$  and Gaussian full-bandwidth at half-height  $\Delta$  are in units of  $\text{cm}^{-1}$ , and  $f_i$  is the corresponding oscillator strength. This expression satisfies the well-known relationship

$$4.32 \times 10^{-9} \int \varepsilon(\omega) d\omega = \sum_i f_i \quad (2)$$

We use  $\Delta = 4000 \text{ cm}^{-1}$  for the optical band broadening to mimic thermal oscillations in dye structures and excitations at room

**Table 1. Comparison of the Excitation Energies  $\omega_l$  in eV and the Corresponding Oscillator Strength  $f_l$  (in Parentheses), Calculated within TDDFT Using Different Exchange-Correlation Functionals, for the Lowest-Energy Excitations of the Experimental Dye DS<sup>a</sup>**

	PBE	B3LYP	CAM-B3LYP	$\omega$ B97X	$\omega$ B97X <sup>b</sup>	expt.
$\omega_0$ ( $f_0$ )	1.84 (0.769)	2.24 (1.231)				
$\omega_1$ ( $f_1$ )	2.66 (1.027)	3.08 (0.570)	2.71 (1.722)	2.90 (1.767)	2.74 (1.855)	2.62–2.90 <sup>c</sup>
$\omega_2$ ( $f_2$ )	2.97 (0.014)	3.53 (0.088)	3.83 (0.015)	4.10 (0.071)	3.97 (0.080)	

<sup>a</sup> Notice that the functionals that do not include a long-range correction (LC), namely PBE and B3LYP, produce a split of the first peak (labeled  $\omega_0$  and  $\omega_1$ ), and the sum of the oscillator strengths of these two peaks is approximately equal to the oscillator strength of the corresponding single peak in the LC functionals CAM-B3LYP and  $\omega$ B97X. <sup>b</sup> Calculated in ethanol solution. <sup>c</sup> In different solutions: acid, 2.62 eV;<sup>27</sup> methanol, 2.79 eV;<sup>27</sup> ethanol, 2.81 eV;<sup>7</sup> acetonitrile, 2.90 eV.<sup>28</sup>

temperature, which is very close to those in experimentally measured absorption spectra.<sup>6–8,10,11</sup>

Before considering the effects of changes in the acceptor group, we examine the reliability of different exchange-correlation functionals available for calculating the electronic and optical properties of these dyes. To this end, we focus on a representative organic dye structure (DS) shown in Figure 1, which is frequently used in experiments<sup>7,27,28</sup> and in modeling,<sup>20,21</sup> and hence the relevant data can be compared at different levels. Table 1 presents the calculated excitation energy and transition oscillator strength for a few lowest excitation channels of DS using different XC functionals in TDDFT. Experimental results, measured in different solutions, are also included. Both the PBE and B3LYP functionals underestimate significantly the first excitation energy and its strength. Long-range-corrected (LC) functionals, such as CAM-B3LYP<sup>18</sup> and  $\omega$ B97X,<sup>19</sup> yield better comparison with experiment. It is known that the solvent effects will lower dye absorption energy<sup>21</sup> by  $\sim 0.1$ – $0.3$  eV; therefore, experimental values quoted in Table 1, which are measured in solution, should be corrected by a similar amount. After the correction it leads to a better agreement with the results from LC-TDDFT calculations on dyes in vacuum. Indeed, by including ethanol solvation in the polarizable continuum model, the first absorption peak is located at 2.74 eV with an oscillator strength of 1.855 using  $\omega$ B97X functional, in good agreement with experiment. Our results are also in good agreement with other calculations, which report the energy for the first absorption peak being 2.28<sup>20</sup> and 2.23 eV<sup>21</sup> in B3LYP functional, 2.97 eV in CAM-B3LYP,<sup>21</sup> and 3.04 eV in  $\omega$ B97X.<sup>20</sup> Minor differences between our results and those from literature are attributed to different computational procedures and parameters used in these approaches. We note that besides dye DS we also compared data on many other similar dyes and found qualitatively the same trend as that for DS. Since the  $\omega$ B97X functional has fewer empirical parameters<sup>19</sup> and shows better agreement with experimental results after the solvent-effect correction, we adopt this functional in the following for predicting optical properties of new dyes. We note that using CAM-B3LYP would yield qualitatively similar results.

Organic dyes with the carboxylate–cyanoacrylic anchoring group have been very successful in real devices.<sup>6–10</sup> From the point of view of electronic structure and optical absorption, it is possible that the side cyano group ( $-\text{CN}$ ) has a positive influence on light absorption and anchoring to the  $\text{TiO}_2$  surface.<sup>29</sup> Accordingly, we begin our investigation with the possibility of replacing  $-\text{CN}$  by other chemical groups and examine the dependence of dye performance on these groups. In Figure 2 we show the set of dye acceptor structures we have investigated. We have replaced the cyano  $-\text{CN}$  group in model

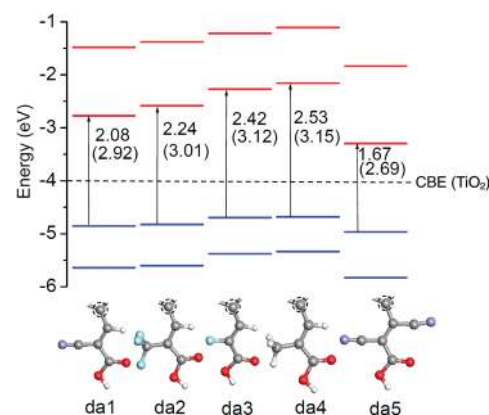


**Figure 2.** Energy levels and corresponding acceptor structures for da1–da5 dyes. Blue and red bars represent occupied and unoccupied orbitals, respectively. Energy gaps between HOMO and LUMO levels calculated from ground-state DFT calculations using the B3LYP exchange-correlation (XC) functional and those from TDDFT using  $\omega$ B97X functional (in parentheses) are indicated besides the arrows for each dye. The horizontal dashed line indicates the level of conduction band edge (CBE) of the anatase  $\text{TiO}_2$  surface in electrolyte solutions ( $-4.0$  eV). Only the atomic structure for the acceptor part of the dyes below the connecting carbon atom (circled) is shown; gray, red, blue, yellow, white, and cyan spheres represent C, O, N, S, H, and F atoms, respectively.

dye da1 by  $-\text{CF}_3$ ,  $-\text{F}$ , and  $-\text{CH}_3$  groups, which are labeled da2, da3, and da4, respectively. Model dye da1, shown in Figure 1, has a very similar structure to that of D21L6 dye synthesized experimentally,<sup>8</sup> except that the hexyl tails at the donor end are replaced by methyl groups. The electronic energy levels of these modified dyes in the ground state are also shown in Figure 2, as calculated using B3LYP/6-31G(d). Compared to the relatively small gap of 2.08 eV for da1, the energy gap is increased by all these modifications. All these changes give a larger energy gap. This may explain the optimal performance in experiment of the cyano CN group as a part of the molecular anchor, which yields the lowest excitation energy favoring enhanced visible light absorption. The spectra with  $\omega$ B97X functional calculated based on eq 1 are shown in Figure 3, and the features for the main peaks of the spectrum are summarized in Table 2. The absorption maximum for da1 is found to locate at 425 nm (2.92 eV) in vacuum and 446 nm (2.78 eV) in ethanol solution (Table 2); the latter is very close to the experimental measured value of 458 nm (2.71 eV) for D21L6 in the same condition,<sup>8</sup> again confirming the validity of our methodology. The extinction coefficients calculated from eq 1 are comparable to experimentally measured



ones<sup>8</sup> after applying an overall scaling factor of  $\sim 0.5$  for the size of the peaks. We found that the first absorption peak is predominantly associated with excitations from the HOMO–1 and HOMO orbitals to the LUMO and LUMO+1 orbitals, with contributions involving other orbitals amounting to less than 15%.

Intuitively, we would expect that the energy levels of the whole dye molecule are modified by the electric field introduced by the presence of side chemical groups on the acceptor, with the changes depending on the electronegativity of these chemical groups: the higher the electronegativity of the group, the lower the energy of the LUMO level, and the smaller the energy gap, assuming the HOMO level, determined by the other (donor) end of the dye, is less influenced by the changes in the acceptor. Our results show that such a simple rule does not apply, considering that –F (in da3) has a higher electronegativity than –CN (in da1)<sup>30</sup> but introduces a larger gap. The changes in electronic structure introduced by substitution of the –CN group by other groups are a result of cooperative effects of both electronegativity and the size and shape of the substituted chemical groups. In close proximity to the backbone and other parts of the anchor, the substituted groups significantly change the local potential that excited electrons will experience. A substituted group that is closer to the backbone and other atoms on the periphery gives rise to a stronger electron repulsion, resulting in a higher energy for the LUMO and a larger gap. This explains why –CH<sub>3</sub>, with an electronegativity very close to that of –CN (2.56 vs 2.69, respectively<sup>30</sup>), has the largest energy gap among the various modifications we considered. Cyano groups introduce a particularly small energy gap due to its linear shape and the fact that electrons placed at the LUMO level are attracted by the end N atom and thus become more delocalized (see discussion on wave functions below).

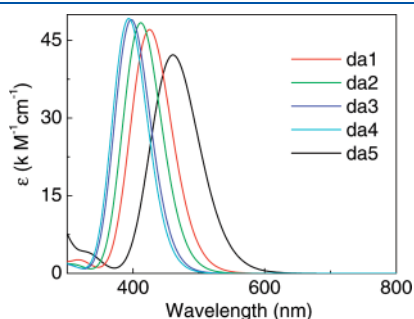


**Figure 3.** Optical absorption spectrum of dyes da1–da5 calculated from TDDFT with  $\omega$ B97X functional.

We did not find any single-group substitution for the –CN that produces a lower energy gap. Therefore we extended our investigation to consider other possibilities. We found that with the substitution of the –H on the backbone by another –CN group, the ground-state energy gap is reduced to 1.67 eV (see Table 2, dye da5). In particular, we emphasize that the LUMO level is still higher by 0.7 V than the conduction band edge (CBE) of anatase TiO<sub>2</sub>, located at  $-4.0$  eV,<sup>31</sup> shown as a dashed line in Figure 2. This would provide enough driving force for ultrafast excited-state electron injection.<sup>29</sup> Another requirement on interface energy level alignment for DSCs to work properly is that the dye HOMO has to be lower than the I<sup>–</sup>/I<sub>3</sub><sup>–</sup> redox potential which is located at about  $-4.8$  eV.<sup>6,7,31</sup> The potential level is comparable to dye HOMOs in Figure 2. However, we note that by comparing calculated energy levels with experimentally measured potential levels, the HOMO and LUMO positions are generally overestimated by  $\sim 0.6$  and  $\sim 0.3$  V, respectively.<sup>6–8</sup> We expect the same trend would occur for dyes discussed in the present work. Taking this correction into account, the new dyes considered would have perfect energy level alignment with respect to the CBE of TiO<sub>2</sub> which are more than 0.4 eV lower than LUMOs, and the I<sup>–</sup>/I<sub>3</sub><sup>–</sup> redox potential is  $\sim 0.5$  V higher than HOMOs, beneficial for DSC applications. In TDDFT calculations with  $\omega$ B97X, da5 has the longest wavelength for maximum absorption among these da-*n* dyes, located at 461 nm, and the corresponding oscillator strength is slightly reduced as compared to the other dyes (Figure 3 and Table 2). We conclude that with the changes considered here on the acceptor group, the HOMO and LUMO levels and optical absorption of the dye can

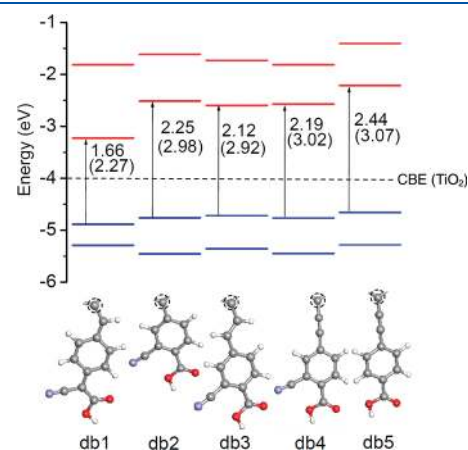


**Figure 4.** Energy levels and corresponding acceptor structures for dyes db1–db5. Conventions are the same as in Figure 2.

**Table 2.** Optical Excitation Energies (in eV), and Corresponding Oscillator Strength (in Parentheses), for the Dyes under Design Obtained from Our First-Principles TDDFT Calculations with the  $\omega$ B97X Functional

		<i>n</i> = 1	<i>n</i> = 2	<i>n</i> = 3	<i>n</i> = 4	<i>n</i> = 5
da- <i>n</i>	$\omega_1$ ( $f_1$ )	2.92 (1.733) <sup>a</sup>	3.01 (1.781)	3.12 (1.804)	3.15 (1.811)	2.69 (1.553)
	$\omega_2$ ( $f_2$ )					3.71 (0.137)
db- <i>n</i>	$\omega_1$ ( $f_1$ )	2.27 (2.443) <sup>b</sup>	2.98 (1.862)	2.92 (2.300)	3.02 (2.240)	3.07 (2.202)
	$\omega_2$ ( $f_2$ )	3.40 (0.130)				
	$\omega_3$ ( $f_3$ )	3.98 (0.275)				
dc- <i>n</i>	$\omega_1$ ( $f_1$ )	2.76 (2.231)	2.71 (2.232)	2.59 (2.137)	2.69 (2.260)	2.37 (2.176) <sup>c</sup>
	$\omega_2$ ( $f_2$ )			3.58 (0.129)		3.53 (0.113)

<sup>a</sup>In ethanol solution: 2.78 (1.802). <sup>b</sup>In ethanol solution: 2.09 (2.491). <sup>c</sup>In ethanol solution: 2.26 (2.227).

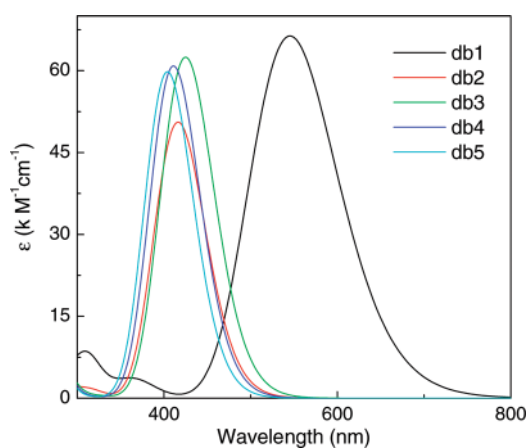


**Figure 5.** Optical absorption spectrum of dyes db1–db5 calculated from TDDFT with  $\omega$ B97X functional.

be gradually tuned as shown in Figures 2 and 3, for optimal performance when used in a real DSC device.

Next, we consider the possibility of incorporating additional spacer groups in the dye acceptor. In particular, we focus on a phenyl ring and its derivatives as the inserted molecular spacer. The dye structures obtained upon additional spacer incorporation, called here db1–db5, are shown in Figure 4. Dye db1 differs from the model dye da1 by inserting a phenyl group between  $-\text{CH}-$  on the backbone and the anchoring carboxylic and cyano groups. The  $-\text{CH}-$  group is removed in db2, with another carbon atom by which carboxylic and cyano groups join also removed. As a result, both the carboxylic and cyano group are now directly bound to the phenyl ring replacing H atoms at respective positions. Dyes db3 and db4 differ from db2 by inserting either a  $-\text{CH}=\text{CH}-$  or a  $-\text{C}\equiv\text{C}-$  group between dithiophene and phenyl groups, respectively. Finally, we replace  $-\text{CN}$  with the normal  $-\text{H}$  termination on the phenyl group (dye db5) to see the effects of cyano group.

Electronic energy levels and optical absorption spectra for this set of dyes are shown in Figures 4 and 5, respectively, and the absorption peak positions are summarized in Table 2. Among this set, the dye db1 stands out for its interesting electronic and optical properties, with the energy gap being rather small (1.55 eV in B3LYP and 2.27 eV in  $\omega$ B97X) and the corresponding oscillator strength being very high (2.443). The absorption maximum corresponds to a long wavelength of 546 nm in TDDFT/ $\omega$ B97X, and it is even longer, 594 nm (2.09 eV), when ethanol solvation effects are taken into account. The oscillator strength of 2.443 (2.491 in ethanol solution) is one of the largest for a single transition among all-organic dyes to our knowledge. For comparison, dye C217 with a high extinction coefficient of  $45 \times 10^3 \text{ M}^{-1} \text{ cm}^{-1}$  at 552 nm has a corresponding oscillator strength of 1.569, with which a striking sunlight-to-electricity efficiency of 9.8% was achieved.<sup>9</sup> Similar behavior occurs for dye DS.<sup>7</sup> Based on these observations we propose that this dye will favor red to infrared light absorption with a very high extinction coefficient. Although its LUMO level ( $-3.23 \text{ eV}$ ) is relatively low compared with other dyes in the same group, it is significantly higher than the conduction band edge of  $\text{TiO}_2$  in solution ( $-4.0 \text{ eV}$ ), even after the 0.3 eV correction discussed earlier. Its HOMO lies below the  $\Gamma^-/\text{I}_3^-$  redox potential. Therefore, with further optimization of the dye/ $\text{TiO}_2$  interfaces, possibly via dipole moment engineering,<sup>32</sup> ultrafast electron injection<sup>29</sup>

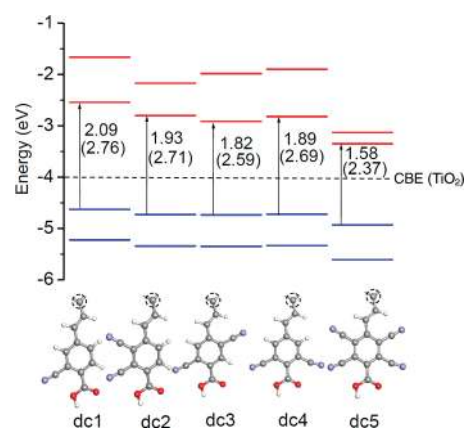


**Figure 6.** Energy levels and corresponding acceptor structures for dyes dc1–dc5. Conventions are the same as in Figure 2.

might be achieved for this dye. This would make dye db1 an attractive candidate for future development of DSC devices, especially for high-extinction, long-wavelength light absorption.

Besides identifying dye db1 as particularly promising, our study also helps elucidate how other modifications in molecular spacer would change dye properties and performance. We found that all other dyes in this set have an optical absorption maximum blue-shifted compared to db1. In particular, compared to db2, the insertion of additional two-carbon groups significantly improves the absorption intensity. Inserting the  $-\text{CH}=\text{CH}-$  group results in better properties than inserting the  $-\text{C}\equiv\text{C}-$  group, since the former produces a higher oscillation strength and a red-shift of the absorption peak (see Figure 5 and Table 2). In addition, the  $-\text{CH}=\text{CH}-$  group may be beneficial also from structural considerations, making the dye molecular structure planar and more rigid. Comparing db4 and db5 clearly shows that adding the  $-\text{CN}$  group to the phenyl spacer introduces desirable features: the energy gap is lowered, and the absorption intensity is enhanced (Table 2).

Since dye db3 has the most desirable features among simpler dyes db2–db5, we chose this structure for further potential improvements: specifically, we systematically analyzed the effects of replacing  $-\text{H}$  by  $-\text{CN}$  groups on the phenyl group of this dye. We constructed a group of new dyes (dc1–dc5) with the only difference between each other being the number and position of the  $-\text{CN}$  group on the phenyl ring in the dye acceptor. We start from a slightly modified db3 dye, dc1, where the dithiophene conductor group is now cross-linked. There is experimental evidence that this cross-linking provides additional benefits in optical absorption;<sup>11</sup> in our calculations we confirmed that dc1 has an even smaller energy gap than db3 (by 0.16 eV in  $\omega$ B97X). The calculated energy levels and optical spectra of this group of dyes upon phenyl  $-\text{CN}$  substitution are shown in Figures 6 and 7, respectively. We found that the gap and optical absorption depends sensitively on the number and position of the  $-\text{CN}$  substitution groups on the phenyl ring. With more  $-\text{CN}$  groups, a smaller energy gap and hence a red-shift in absorption maximum from 449 nm (with 1  $-\text{CN}$ ) to 523 nm (with 4  $-\text{CN}$ ) is observed. The absorbance intensity is less sensitive to  $-\text{CN}$  substitution, with minor changes from case to case. The absorption also depends on the position of the  $-\text{CN}$  groups. We place the  $-\text{CN}$  far from the binding carboxylic group, which results in a more delocalized electron density distribution (not shown);

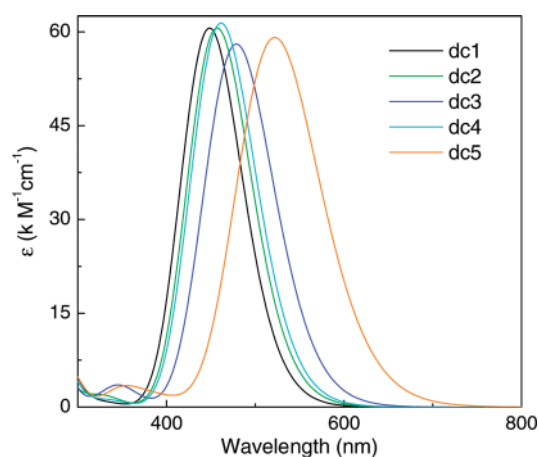


Figure 7. Optical absorption spectrum of dyes dc1–dc5 calculated from TDDFT with  $\omega$ B97X functional.

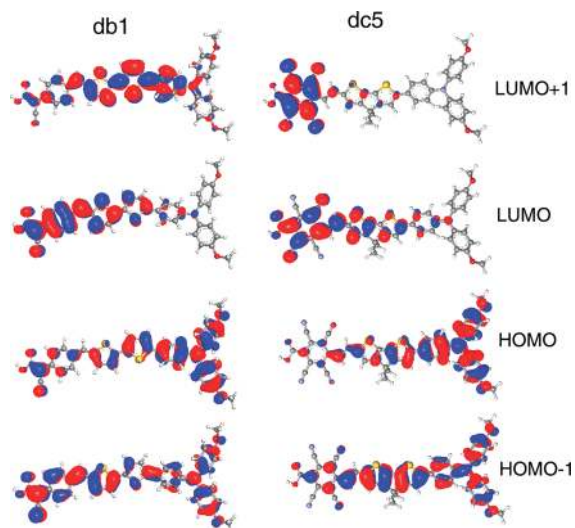


Figure 8. Wave function plots for the representative dye db1 (left column) and dc5 (right column). Four orbitals, HOMO–1, HOMO, LUMO, and LUMO+1, which contribute most to visible-light absorption, are shown for each dye.

therefore, the energy gap is slightly lowered by 0.06 eV compared to dc1. For all cases of two –CN groups substitution (dc2–dc4), the diagonal arrangement of the two –CN groups on the benzenoid ring as in dc3 has the smallest gap and strength (2.59 eV and 2.137 in  $\omega$ B97X), while putting two –CN groups at immediate neighboring sites to the carboxyl group as in dc4 introduces a large gap and the highest strength (2.69 eV and 2.260 in  $\omega$ B97X). We also considered the arrangement of both two CN groups away from the carboxyl group, which produce similar results (not shown). We note that the results on these minor structural variations are sensitive to the XC functional used; slightly different orderings are obtained with the less accurate B3LYP functional. The question of which one produces results closer to reality is of interest and subject to future experimental confirmations.

With all four H atoms on the phenyl ring replaced by –CN groups, the dye yields a small gap (2.37 eV) and retains a high strength (2.176). In ethanol solution, the calculated absorption

maximum and corresponding oscillator strength is 2.26 eV (547 nm) and 2.227. Again this is very promising for long-wavelength absorption, similar to the case of db1. To further elucidate the electronic properties for these two promising dyes, we show in Figure 8 the wave function plots for the molecular orbitals HOMO–1, HOMO, LUMO, and LUMO+1 of dyes db1 and dc5. Clearly, the occupied states are mainly distributed around the donor part of the molecules, and the unoccupied ones are mainly localized in the acceptor group, confirming the charge-transfer nature of low-energy excitations in these dyes. Furthermore, in both cases we find that the –CN groups, particularly the N-atom end, help to delocalize electronic clouds on the dye acceptor, reducing electron repulsion and LUMO levels. This is most pronounced in dc5; the resulting LUMO states are strongly localized at the acceptor end, with little overlap with HOMOs, which would facilitate electron injection and slow down electron back transfer, both advantageous for DSC applications. Compared to dye db1, dc5 possesses a simpler, more uniform acceptor structure. Since there are no complicated substructures at the connecting –CH– and the end C atom bound to cyanoacrylic and carboxylic groups as in db1, we expect that the synthesis of dc5 might be easier to achieve in experiment.

In conclusion, we have employed accurate first-principles calculations based on long-range-corrected TDDFT calculations to investigate a series of novel acceptor groups for donor- $\pi$ -acceptor type dyes. We found that upon modifications on the dye acceptor group, the dye electronic levels relative to TiO<sub>2</sub> conduction bands and corresponding optical absorption properties can be tuned gradually. This allows dye optimization to maximize DSC device performance under various experimental conditions. Our calculations reveal the nature of cooperative effects of the electronegativity and the size/shape of chemical groups to influence dye absorption and redox potential levels. In particular, we propose that the model dye db1, with the insertion of an additional phenyl spacer in the acceptor group relative to the experimentally investigated dye JK2,<sup>6</sup> and the dye dc5 with a CN-substituted phenyl group, might be promising candidates for red to infrared light absorption, which may offer improved sunlight-to-electricity conversion efficiency when used alone or in combination with other dyes. Our study opens a way for material design of new dyes with target properties to advance the performance of organic dye solar cells.

## AUTHOR INFORMATION

### Corresponding Author

\*E-mail: smeng@iphy.ac.cn; Tel: +86-10-82649396; Fax: +86-10-82649228.

## ACKNOWLEDGMENT

We are thankful for helpful discussions with F. Rotzinger and S. Zakeeruddin. S.M. acknowledges financial support from NSFC (No. 11074287) and the hundred-talent program and knowledge innovation project of CAS.

## REFERENCES

- (1) O'Regan, B.; Grätzel, M. *Nature* **1991**, 353, 737–740.
- (2) Grätzel, M. *Chem. Lett.* **2005**, 34, 8–13.
- (3) Grätzel, M. *Acc. Chem. Res.* **2009**, 42, 1788–1798.
- (4) Horiuchi, T.; Miura, H.; Uchida, S. *Chem. Commun.* **2003**, 3036.

- (5) Ito, S.; Zakeeruddin, S. M.; Humphry-Baker, R.; Liska, P.; Charvet, R.; Pascal, C.; Nazeeruddin, M. K.; Pechy, P.; Takata, M.; Miura, H.; Uchida, S.; Grätzel, M. *Adv. Mater.* **2006**, *18*, 1202–1205.
- (6) Kim, S.; Lee, J. K.; Kang, S. O.; Ko, J.; Yum, J. H.; Fantacci, S.; De Angelis, F.; Di Censo, D.; Nazeeruddin, M. K.; Grätzel, M. *J. Am. Chem. Soc.* **2006**, *128*, 16701–16707.
- (7) Hagberg, D. P.; Yum, J. H.; Lee, H. J.; De Angelis, F.; Marinado, T.; Karlsson, K. M.; Humphry-Baker, R.; Sun, L.; Hagfeldt, A.; Grätzel, M.; Nazeeruddin, M. K. *J. Am. Chem. Soc.* **2008**, *130*, 6259–6266.
- (8) Yum, J. H.; Hagberg, D. P.; Moon, S. J.; Karlsson, K. M.; Marinado, T.; Sun, L.; Hagfeldt, A.; Nazeeruddin, M. K.; Grätzel, M. *Angew. Chem., Int. Ed.* **2009**, *48*, 1576–1580.
- (9) Zhang, G.; Bala, H.; Cheng, Y.; Shi, D.; Lv, X.; Yu, Q.; Wang, P. *Chem. Commun.* **2009**, 2198–2200.
- (10) Xu, M.; Wenger, S.; Bala, H.; Shi, D.; Li, R.; Zhou, Y.; Zakeeruddin, S. M.; Grätzel, M.; Wang, P. *J. Phys. Chem. C* **2009**, *113*, 2966–2973.
- (11) Zeng, W. D.; Cao, Y. M.; Bai, Y.; Wang, Y. H.; Shi, Y. S.; Zhang, M.; Wang, F. F.; Pan, C. Y.; Wang, P. *Chem. Mater.* **2010**, *22*, 1915–1925.
- (12) Duncan, W. R.; Prezhdo, O. V. *Annu. Rev. Phys. Chem.* **2007**, *58*, 143–184.
- (13) Meng, S.; Ren, J.; Kaxiras, E. *Nano Lett.* **2008**, *8*, 3266–3272.
- (14) Kohn, W.; Sham, L. J. *Phys. Rev.* **1965**, *140*, A1133–A1138.
- (15) Runge, E.; Gross, E. K. U. *Phys. Rev. Lett.* **1984**, *52*, 997.
- (16) Dreuw, A.; Head-Gordon, M. *J. Am. Chem. Soc.* **2004**, *126*, 4007–4016.
- (17) Ikura, H.; Tsuneda, T.; Yanai, T.; Hirao, K. *J. Chem. Phys.* **2001**, *115*, 3540–3544.
- (18) Yanai, T.; Tew, D. P.; Handy, N. C. *Chem. Phys. Lett.* **2004**, *393*, 51–57.
- (19) Chai, J.-D.; Head-Gordon, M. *J. Chem. Phys.* **2008**, *128*, 084106.
- (20) Casanova, D.; Rotzinger, F. P.; Grätzel, M. *J. Chem. Theory Comput.* **2010**, *6*, 1219–1227.
- (21) Pastore, M.; Mosconi, E.; De Angelis, F.; Grätzel, M. *J. Phys. Chem. C* **2010**, *114*, 7205–7212.
- (22) Soler, J. M.; Artacho, E.; Gale, J. D.; Garcia, A.; Junquera, J.; Ordejon, P.; Sanchez-Portal, D. *J. Phys.: Condens. Matter* **2002**, *14*, 2745–2779.
- (23) Frisch, M. J.; *Gaussian 09*; Gaussian Inc.: Wallingford, CT, 2009.
- (24) Troullier, N.; Martins, J. L. *Phys. Rev. B* **1991**, *43*, 1993–2006.
- (25) Perdew, J. P.; Burke, K.; Ernzerhof, M. *Phys. Rev. Lett.* **1996**, *77*, 3865–3868.
- (26) Cossi, M.; Barone, V. *J. Chem. Phys.* **2001**, *115*, 4708–4717.
- (27) Hagberg, D. P.; Edvinsson, T.; Marinado, T.; Boschloo, G.; Hagfeldt, A.; Sun, L. C. *Chem. Commun.* **2006**, 2245–2247.
- (28) Hagberg, D. P.; Marinado, T.; Karlsson, K. M.; Nonomura, K.; Qin, P.; Boschloo, G.; Brinck, T.; Hagfeldt, A.; Sun, L. *J. Org. Chem.* **2007**, *72*, 9550–9556.
- (29) Meng, S.; Kaxiras, E. *Nano Lett.* **2010**, *10*, 1238–1247.
- (30) Boyd, R. J.; Edgecombe, K. E. *J. Am. Chem. Soc.* **1988**, *110*, 4182–4186.
- (31) Kavan, L.; Grätzel, M.; Gilbert, S. E.; Klemenz, C.; Scheel, H. J. *J. Am. Chem. Soc.* **1996**, *118*, 6716–6723.
- (32) Chen, P.; Yum, J. H.; De Angelis, F.; Mosconi, E.; Fantacci, S.; Moon, S.-J.; Baker, R. H.; Ko, J.; Nazeeruddin, M. K.; Grätzel, M. *Nano Lett.* **2009**, *9*, 2487–2492.